



HAL
open science

Long-Term Effects of Early-Life Antibiotic Exposure on Resistance to Subsequent Bacterial Infection

Claire Roubaud-Baudron, Victoria Ruiz, Alexander Swan, Bruce Vallance, Ceren Ozkul, Zhiheng Pei, Jackie Li, Thomas Battaglia, Guillermo Perez-Perez, Martin Blaser

► **To cite this version:**

Claire Roubaud-Baudron, Victoria Ruiz, Alexander Swan, Bruce Vallance, Ceren Ozkul, et al.. Long-Term Effects of Early-Life Antibiotic Exposure on Resistance to Subsequent Bacterial Infection. *mBio*, 2019, 10 (6), pp.e02820-19. 10.1128/mBio.02820-19 . inserm-03010065

HAL Id: inserm-03010065

<https://inserm.hal.science/inserm-03010065>

Submitted on 17 Nov 2020

HAL is a multi-disciplinary open access archive for the deposit and dissemination of scientific research documents, whether they are published or not. The documents may come from teaching and research institutions in France or abroad, or from public or private research centers.

L'archive ouverte pluridisciplinaire **HAL**, est destinée au dépôt et à la diffusion de documents scientifiques de niveau recherche, publiés ou non, émanant des établissements d'enseignement et de recherche français ou étrangers, des laboratoires publics ou privés.



Long-Term Effects of Early-Life Antibiotic Exposure on Resistance to Subsequent Bacterial Infection

Claire Roubaud-Baudron,^{a,b,c} Victoria E. Ruiz,^{c,d} Alexander M. Swan, Jr.,^c Bruce A. Vallance,^e Ceren Ozkul,^{c,f} Zhiheng Pei,^g Jackie Li,^c Thomas W. Battaglia,^c Guillermo I. Perez-Perez,^c  Martin J. Blaser^{c,h}

^aCHU Bordeaux, Pôle de Gérontologie Clinique, Bordeaux, France

^bUniversity of Bordeaux, INSERM, UMR1053 Bordeaux Research in Translational Oncology, BaRITOn, Bordeaux, France

^cDepartment of Medicine, New York University Langone Medical Center, New York, New York, USA

^dDepartment of Biology, St. Francis College, Brooklyn, New York, USA

^eDivision of Gastroenterology, Department of Pediatrics, University of British Columbia, Vancouver, British Columbia, Canada

^fDepartment of Pharmaceutical Microbiology, Hacettepe University School of Pharmacy, Ankara, Turkey

^gDepartment of Pathology, New York University Langone Medical Center, New York, New York, USA

^hCenter for Advanced Biotechnology and Medicine, Rutgers University, New Brunswick, NJ, USA

ABSTRACT Early-life antibiotic exposure may provoke long-lasting microbiota perturbation. Since a healthy gut microbiota confers resistance to enteric pathogens, we hypothesized that early-life antibiotic exposure would worsen the effects of a bacterial infection encountered as an adult. To test this hypothesis, C57BL/6 mice received a 5-day course of tylosin (macrolide), amoxicillin (β -lactam), or neither (control) early in life and were challenged with *Citrobacter rodentium* up to 80 days thereafter. The early-life antibiotic course led to persistent alterations in the intestinal microbiota and even with pathogen challenge 80 days later worsened the subsequent colitis. Compared to exposure to amoxicillin, exposure to tylosin led to greater disease severity and microbiota perturbation. Transferring the antibiotic-perturbed microbiota to germfree animals led to worsened colitis, indicating that the perturbed microbiota was sufficient for the increased disease susceptibility. These experiments highlight the long-term effects of early-life antibiotic exposure on susceptibility to acquired pathogens.

IMPORTANCE The gastrointestinal microbiota protects hosts from enteric infections; while antibiotics, by altering the microbiota, may diminish this protection. We show that after early-life exposure to antibiotics host susceptibility to enhanced *Citrobacter rodentium*-induced colitis is persistent and that this enhanced disease susceptibility is transferable by the antibiotic-altered microbiota. These results strongly suggest that early-life antibiotics have long-term consequences on the gut microbiota and enteropathogen infection susceptibility.

KEYWORDS *Citrobacter rodentium*, pathogen-induced colitis, gastrointestinal microbiota, host resistance, murine model, bioluminescence, colonic inflammation, antibiotics

The gastrointestinal tract carries highly complex and dense microbial populations (1–3), known to have important beneficial functions, including nutrient absorption, vitamin synthesis, and protection against pathogens (4). The microbiota protects the host from pathogen invasion either directly, by producing antimicrobial substances or competing for nutrients or space, or indirectly, by eliciting mucosal immune responses (5–7).

Antibiotics affect gut microbiota composition (8, 9). Studies since the 1950s have shown that exposure of mice to antibiotics prior to experimental inoculation with *Salmonella* worsens outcome (10, 11). In humans, antibiotic exposure enhances sus-

Citation Roubaud-Baudron C, Ruiz VE, Swan AM, Jr, Vallance BA, Ozkul C, Pei Z, Li J, Battaglia TW, Perez-Perez GI, Blaser MJ. 2019. Long-term effects of early-life antibiotic exposure on resistance to subsequent bacterial infection. *mBio* 10:e02820-19. <https://doi.org/10.1128/mBio.02820-19>.

Editor Pascale F. Cossart, Institut Pasteur

Copyright © 2019 Roubaud-Baudron et al. This is an open-access article distributed under the terms of the [Creative Commons Attribution 4.0 International license](https://creativecommons.org/licenses/by/4.0/).

Address correspondence to Martin J. Blaser, Martin.Blaser@cabm.rutgers.edu.

This article is a direct contribution from Martin J. Blaser, a Fellow of the American Academy of Microbiology, who arranged for and secured reviews by Eric Pamer, University of Chicago, and Joshua Fierer, VA San Diego & UC San Diego School of Medicine.

Received 26 October 2019

Accepted 1 November 2019

Published 24 December 2019

ceptibility to *Clostridium difficile* infection (12). These observations suggest that antibiotic exposure, by perturbing the composition of the host microbiota, may directly influence the severity of enteric infections. Such model studies have largely been conducted in adult animals in which pathogen exposure follows closely after the antibiotic course has ended (7, 13, 14).

Sharing host-interactive mechanisms with certain pathogenic strains of *Escherichia coli* (15), *Citrobacter rodentium* is a mouse-restricted Gram-negative bacterium that induces colitis (16, 17). The severity and consequences of *C. rodentium* infection are affected by the host strain genetic background: while NIH or C57BL/6 mice develop diarrhea and weight loss, these ill effects are transient (18) and the mice develop resistance against subsequent infections (19), whereas C3H-HeJ mice suffer high mortality (20). Interstrain variation in host microbiota composition also influences the outcome of *C. rodentium* infection (14, 21–23). That transferring host microbiota from resistant to susceptible mouse strains or vice versa affects mortality (21, 23, 24) indicates that the composition of the host microbiota affects disease outcome. In particular, specific commensals, e.g., segmented filamentous bacteria (“*Candidatus* Savagella”), augment resistance to *C. rodentium* (22), influencing its colonic colonization (25). Conversely, exposure of adult mice to metronidazole, an antimicrobial with broad antianaerobic activity, led to more severe *C. rodentium* infection (14).

In both mice (26) and humans (27), early life is the crucial period for the development of the mature adult microbiome. Consequently, exposure to antibiotics early in life may induce long-term alterations in the diversity, composition, and metagenomic content of the microbiota (28), even following a single antibiotic course (29, 30), and the antibiotic-induced selection of the microbiota was both necessary and sufficient for changing immunological development (30).

All over the world, young children are receiving multiple antibiotic courses, often inappropriately for mild and self-limiting conditions (31). Although epidemiologic studies provide evidence that such exposures during early life may increase susceptibility to subsequent infections (32, 33), this hypothesis has not yet been directly tested experimentally. Therefore, we examined the effects of a single early-life antibiotic course on the characteristics of subsequent pathogen challenge. We found that early-life antibiotic exposure worsened the outcome of *C. rodentium* infection in adult life and that the perturbed microbiota was sufficient for transferring the enhanced effect to antibiotic-naïve recipient mice.

RESULTS

Exposure to tylosin accelerates the course of *C. rodentium* infection when mice are challenged 1 day after stopping the antibiotic. To determine whether antibiotic exposure can affect host resistance even after it is no longer being administered, we challenged young adult mice with *C. rodentium* immediately after a 5-day tylosin (macrolide) course was completed; control mice were unexposed to tylosin and/or inoculated with Luria broth (LB) rather than *C. rodentium* (Fig. 1A). All uninfected mice gained weight over time (Fig. 1B; see also Fig. S1E in the supplemental material), whereas all infected mice lost weight (Fig. 1B); however, among infected mice, those that had been exposed to tylosin started losing weight ~5 days earlier than antibiotic-naïve mice. Two infected antibiotic-naïve mice died 9 days postinfection (dpi), and all remaining infected mice were sacrificed at 11 dpi due to excessive weight loss. Fecal occult blood was absent in uninfected mice but among infected mice was present ~1 day earlier and more frequently in those that had been exposed to tylosin than in the antibiotic-naïve mice (Fig. 1C). Among infected mice, those that had been tylosin exposed had higher fecal and *in vivo* *C. rodentium* levels from 1 to 4 dpi than did the antibiotic-naïve mice (Fig. 1D to F). Specific IgM antibodies were absent in the sera of mice prior to *C. rodentium* challenge and were absent at all times in uninfected mice (Fig. 1G). At 7 dpi, specific IgM levels were higher in mice exposed to tylosin than in antibiotic-naïve mice (0.80 ± 0.060 versus 0.23 ± 0.012 ; $P = 0.015$). By the day of sacrifice (11 dpi), IgM levels became similar in both groups of infected mice, whether

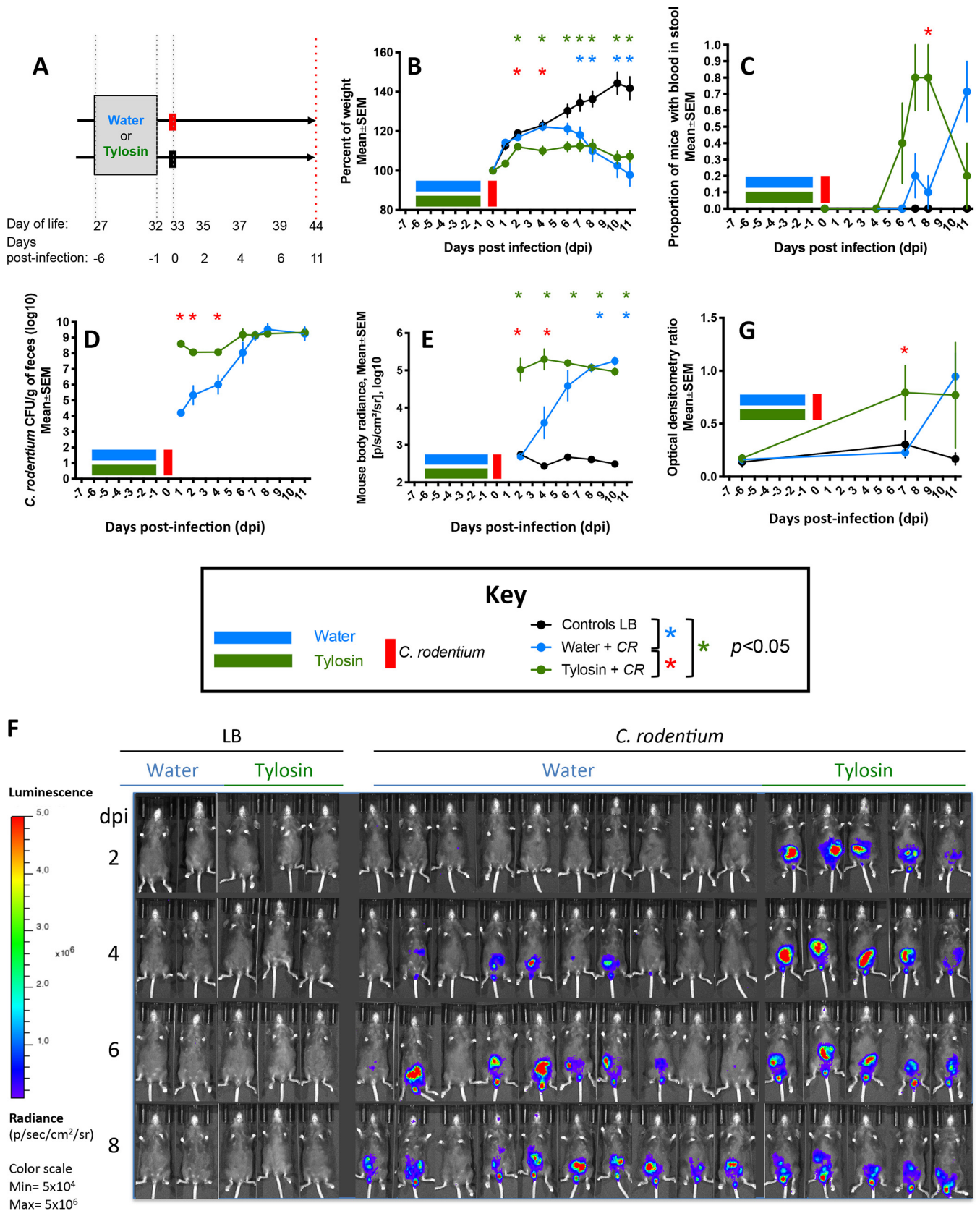


FIG 1 Characteristics of mice challenged with *C. rodentium* (or Luria broth) 1 day after stopping tylosin or water. (A) Study design. Twenty-one-day-old mice received a 5-day course of tylosin ($n = 8$) or water ($n = 12$). The following day, mice from both treatment groups were challenged by *luxCDABE C. rodentium* (CR) (water + CR [$n = 10$; blue] or tylosin + CR [$n = 5$; green]) or Luria broth (LB) (water + LB [$n = 2$] or tylosin + LB [$n = 3$]; black). The group treated with (Continued on next page)

tylosin exposed or not (Fig. 1G). Specific serum IgG was absent throughout the brief experimental course in all mice (data not shown). This experiment confirmed prior studies indicating that in adult mice, proximate antibiotic exposure worsens subsequent pathogen challenge (14).

Effects of tylosin exposure and subsequent *C. rodentium* challenge on microbiota. In the model system with adult mice, we next sought to assess how substantially the tylosin exposure affected the gastrointestinal microbiota. Tylosin exposure significantly decreased community richness (Fig. 2A) and affected community structure (β -diversity) (Fig. 2B), as we now expected (28, 30). Tylosin exposure decreased the relative abundances of certain anaerobes (e.g., *Bacteroidetes* and *Tenericutes*) and increased *Proteobacteria* (Fig. 2C). Among tylosin-exposed mice, *C. rodentium* challenge transiently (2 dpi) increased α -diversity ($P < 0.001$) (Fig. 2A). The *C. rodentium* challenge further affected β -diversity, but these effects appeared earlier (4 dpi) in the tylosin-exposed mice (Fig. 2B). This experiment indicates that in adult mice, both the tylosin exposure and *C. rodentium* challenge affect microbiota community richness and structure, with effects persisting until the time of sacrifice in this acute infection model.

Mice exposed to early-life antibiotics develop enhanced colitis when challenged 23 days later with *C. rodentium*. With the development of the experimental system and phenotype measurement in our lab, we now could examine whether early-life antibiotic exposure would influence the course of infection in young adults (33 days of life). In this experiment, nursing dams were exposed to one of two different antibiotics (tylosin or amoxicillin) in their drinking water or not (control) when their pups were 5 to 10 days old. The pups were exposed to therapeutic doses of the antibiotics through their mothers' milk (28, 30) and at P33 (23 days later) were challenged with *C. rodentium* or LB (as a control) (Fig. 3A). The antibiotic exposures did not significantly affect immediate survival and weight loss (Fig. 3B and C). However, the early-life-tylosin-exposed mice were more susceptible than the antibiotic-naive mice to *C. rodentium* invasion immediately following challenge (Fig. 3E and F and Fig. S2A). Amoxicillin exposure worsened colitis severity with increased fecal blood (Fig. 3D). At P44, 34 days after the early-life antibiotic exposure had ceased, the mice exposed to either of the antibiotics had more severe colonic tissue injury from the *C. rodentium* challenge than did the antibiotic-naive mice (Fig. 3G and H). Among the challenged mice, those exposed to tylosin had a significantly lower proportion of colonic T_H17 cell levels at sacrifice than did the antibiotic-naive mice; the total number of colonic T_H17 cells followed the same trend (Fig. 3I and Fig. S3). Among infected mice, there were no significant differences in the frequencies of regulatory (Foxp3⁺) T cells, or T_H1 (CD4⁺ IFN- γ ⁺) cells, between the exposure groups (data not shown).

Both prior to and following *C. rodentium* challenge, early-life tylosin exposure significantly reduced intestinal α -diversity compared to that of antibiotic-naive mice, while amoxicillin exposure had an intermediate effect (Fig. 4A and B). After the early-life exposures, microbial populations remained skewed for at least the next 23 days (Fig. 4C and D) and following *C. rodentium* challenge (Fig. 4E). Compared to uninfected mice, those challenged with *C. rodentium* developed higher *Proteobacteria* abundances, as reported previously (34), whether the mice had been exposed to antibiotics or not (Fig. 4E). Among the tylosin-exposed mice, those challenged with *C. rodentium* had lower abundances of an unidentified *Bacteroidetes* S24-7 family member than those that were uninfected (Fig. 4E). This experiment indicates that 23 days following early-life antibiotic exposure, the host microbiota remained perturbed and that *C. rodentium* challenge induced more severe infection in these young adult animals that had received either antibiotic in early life.

FIG 1 Legend (Continued)

water plus CR consisted of 5 mice each that received one or two CR gavages (see Fig. S1A to D). Fecal pellets were collected before and after antibiotic exposure and challenge, and bioluminescence was imaged every 2 days after infection. All mice were sacrificed 11 days postinfection. (B) Body weight over time, calculated as a percentage of prechallenge weight. (C) Proportion of mice with fecal occult blood. (D) Quantitation of *C. rodentium* in fecal culture. (E) Quantitation of *C. rodentium* by *in vivo* bioluminescent imaging. (F) *In vivo* bioluminescent images of mouse bodies. (G) Anti-*C. rodentium* IgM antibody levels.

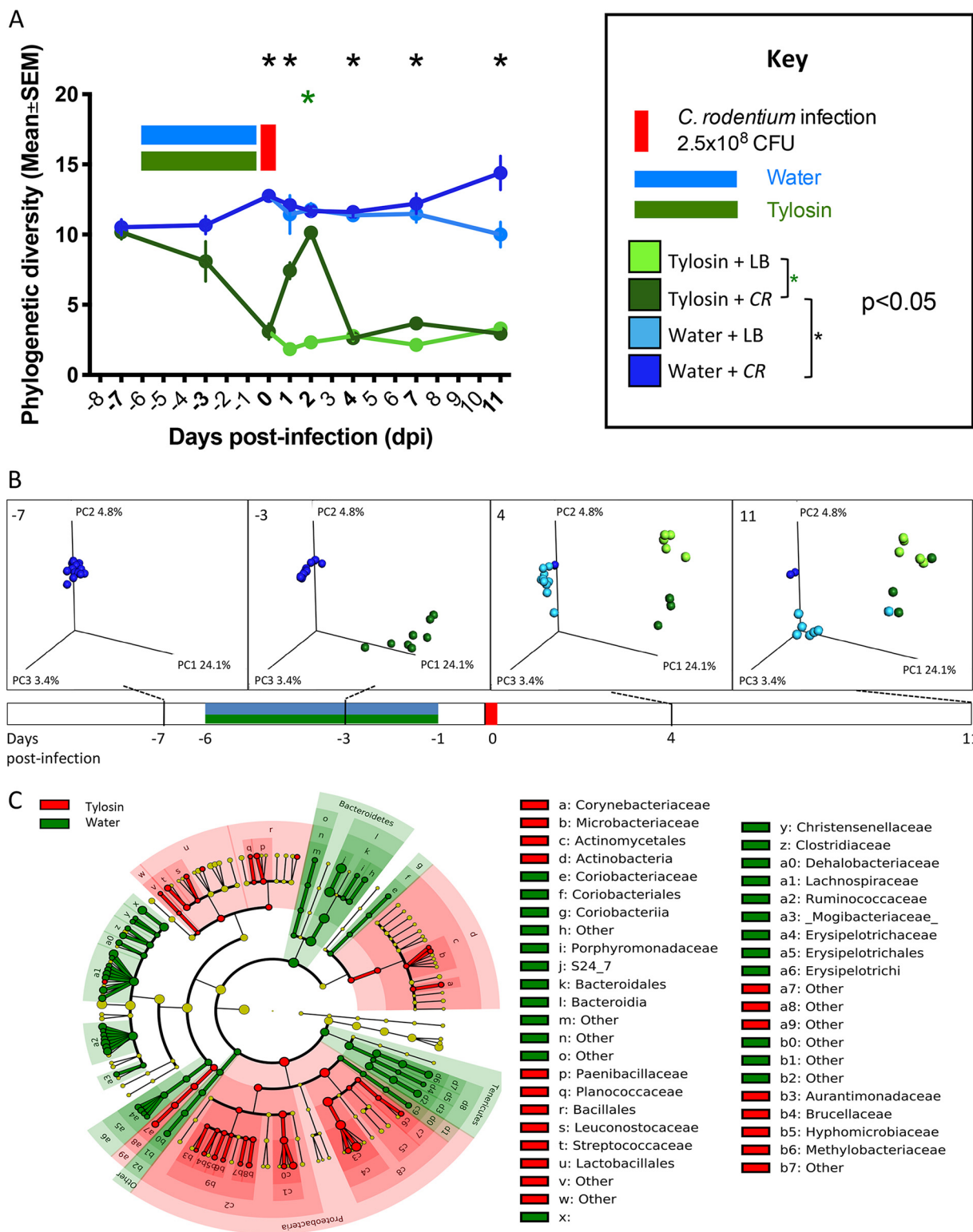


FIG 2 Gut microbiota characteristics of mice challenged with *C. rodentium* (or LB) 1 day after stopping tylosin (or water). For the study design, see the legend to Fig. 1A. (A) α -diversity in fecal samples. Using the phylogenetic diversity (PD whole tree) metric, α -diversity was measured in fecal samples obtained at the times pre- and postinfection shown in bold. Mice were exposed to tylosin (or water) and then challenged with CR (or LB). (B) Unweighted UniFrac analysis of fecal specimens from four time points visualized by principal-coordinate analysis (PCoA) (for statistical significance, see Table S1). The three components explain 32.3% of the total variance, and the colors are as in panel A. (C) LefSe analysis, with cladogram showing significantly differential taxa between tylosin- and water-exposed mice at day 0, immediately prior to infection. Shading indicates significant overrepresentation of the indicated taxa ($P < 0.05$; LDA [linear discriminant analysis] > 2).

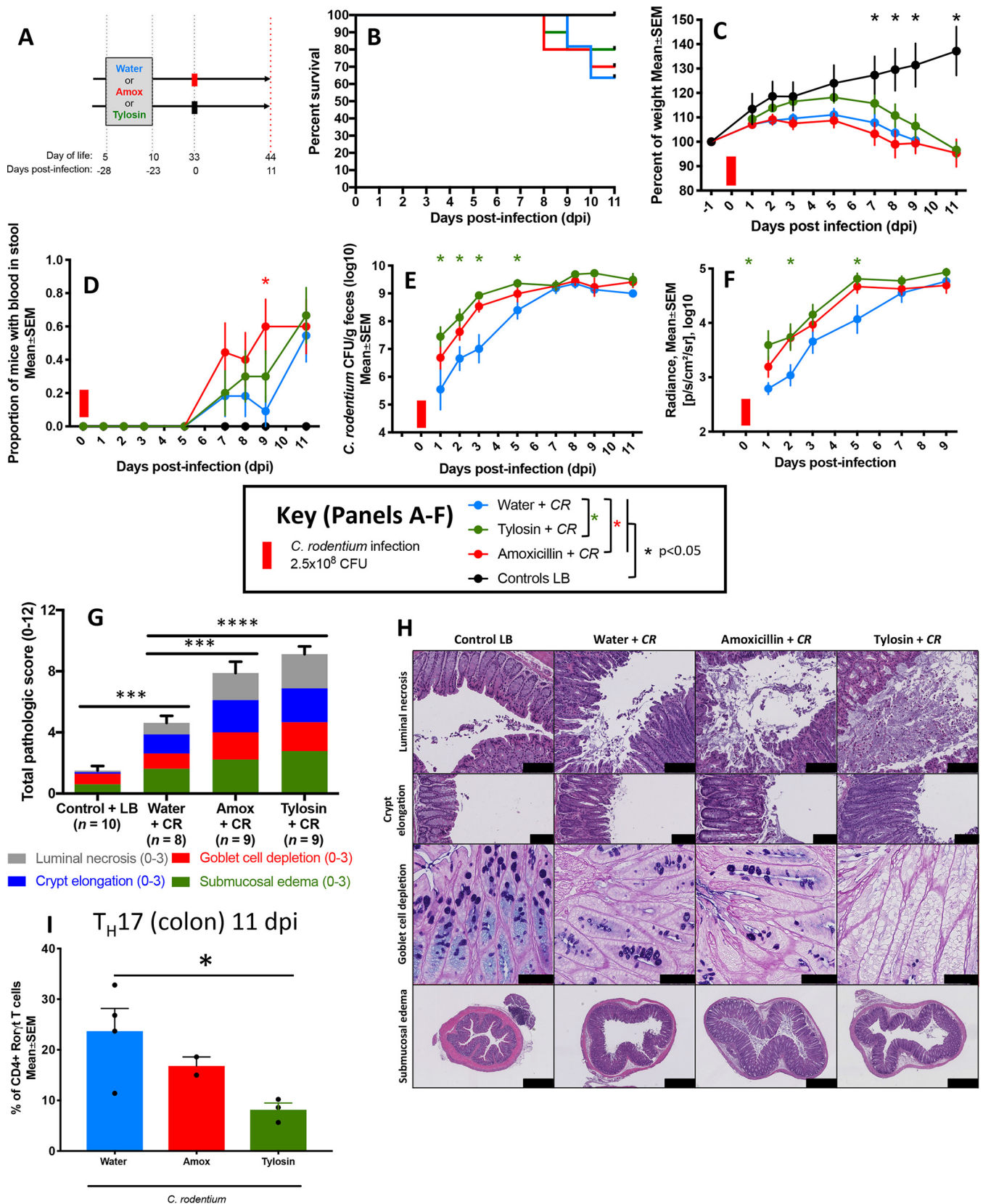


FIG 3 Characteristics of mice challenged with *C. rodentium* (or LB) 23 days after antibiotic or water exposure. (A) Study design. Five-day-old pups received a 5-day course of tylosin ($n = 13$), amoxicillin ($n = 13$), or water ($n = 15$). Twenty-three days later, pups were challenged with *luxCD456* *C. rodentium* (water + CR [$n = 11$; blue]), tylosin + CR [$n = 10$; green], or amoxicillin + CR [$n = 10$; red]) or with LB (as a control) (water + LB [$n = 4$], tylosin + LB [$n = 3$], or amoxicillin + LB [$n = 3$]; black). (B) Percent surviving by exposure group. (C) Body weight over time, calculated as a percentage of prechallenge weight. For the water group,

(Continued on next page)

Mice exposed to early-life antibiotics develop enhanced colitis when challenged with *C. rodentium* as adults, 80 days later. Since the consequences of early-life antibiotics may persist into adulthood (28, 30, 35), we next examined the severity of *C. rodentium*-induced colitis exactly as before, but now the interval to pathogen challenge was 80 days and mice were sacrificed 12 days postchallenge (Fig. 5A). Compared to that of the antibiotic-naïve mice, those exposed to antibiotics trended toward decreased survival ($P = 0.07$ for the antibiotic groups combined, log rank test) (Fig. 5B) and showed greater weight loss during *C. rodentium* infection (Fig. 5C). The mice exposed to tylosin in early life more frequently had fecal occult blood (Fig. 5D) and had higher fecal *C. rodentium* loads (Fig. 5E), higher cecal and colonic *C. rodentium* counts (Fig. 5F), and higher *in vivo* *C. rodentium* levels (Fig. 5G and Fig. S2B). The antibiotic-exposed mice developed higher IgM responses to *C. rodentium* infection than the antibiotic-naïve mice (Fig. 4H and I). Among the *C. rodentium*-infected mice, those exposed to antibiotics had more extensive colonic tissue injury (which was more severe in tylosin-exposed mice than amoxicillin-exposed mice) than did antibiotic-naïve mice (Fig. 5J and K).

Seventy-eight days following the antibiotic exposure and 2 days prior to *C. rodentium* or LB (control) inoculation, the exposed mice significantly differed from the antibiotic-naïve mice in both microbial community structure (β -diversity) (Fig. 6A) and taxon composition (Fig. 6B and C), confirming that a single early-life antibiotic course had long-lasting effects on the host's microbiota (28, 30). *C. rodentium* challenge further affected β -diversity (Fig. 6A). Both prior to and following *C. rodentium* challenge, early-life tylosin exposure significantly reduced gastrointestinal α -diversity compared to that of antibiotic-naïve mice, while amoxicillin exposure had an intermediate effect (Fig. 6D to F). This experiment reveals that early-life antibiotic exposure has effects on both host microbiota and subsequent *C. rodentium* infection severity in adult mice.

The antibiotic-perturbed microbiota transfers enhanced susceptibility to colitis after subsequent *C. rodentium* challenge. In prior studies, the antibiotic-perturbed microbiota harvested 2 days after tylosin exposure ceased was sufficient to transfer immunological phenotypes to germfree mice (30). We now sought to examine whether the antibiotic-perturbed microbiota, in the current models, would lead to differential responses to *C. rodentium* challenge. To this end, we harvested the cecal contents of 32-day-old mice that had received tylosin or not (control) between days 5 and 10 of life. We then gavaged 6-week-old germfree mice with these tylosin-perturbed or control cecal contents and 5 days later challenged them with *C. rodentium* (Fig. 7A). Mice were sacrificed at 9 dpi since by this time, recipients of the tylosin-perturbed microbiota had experienced substantial weight loss compared to that of controls (Fig. 7B). Recipients of the tylosin-perturbed microbiota also suffered more severe colitis than did controls, with more frequent fecal occult blood ($P = 0.026$, log rank test) (Fig. 7C) and more extensive colonic tissue injury (Fig. 7D and E). Fecal *C. rodentium* levels, but not *in vivo* *C. rodentium* levels, trended higher in the recipients of the perturbed microbiota (Fig. 7F and G).

Compared to that in the control microbiota recipients, α -diversity in fecal specimens obtained both prior to and following *C. rodentium* challenge was decreased in the recipients of the tylosin-perturbed microbiota (Fig. 8A) and in their colonic and cecal contents obtained at sacrifice (Fig. 8B). The fecal microbiota of the two groups differed significantly in β -diversity, and the cecal microbiota showed specific taxonomic differences, which persisted after the *C. rodentium* challenge (Fig. 8C and D). This experiment

FIG 3 Legend (Continued)

analysis was censored at day 11 due to multiple deaths. (D) Proportion of mice with fecal occult blood. (E) Quantitation of *C. rodentium* in fecal culture. (F) Quantitation of *C. rodentium* by *in vivo* bioluminescent imaging. (G) Cumulative histopathology scores (means \pm SEM), calculated by evaluating luminal necrosis, crypt elongation, goblet cell depletion, and submucosal edema. ***, $P < 0.01$; ****, $P < 0.0001$. (H) Representative H&E-stained (or, in the third row, AB/PAS-stained) distal colonic sections (scale bars: for luminal necrosis, 100 μ m; for crypt elongation, 100 μ m; for goblet cell depletion, 50 μ m; and for submucosal edema, 500 μ m). (I) Flow cytometric analysis of colonic CD4⁺ cells after tylosin, amoxicillin, or water exposure and subsequent *C. rodentium* challenge. Populations were gated on live CD45⁺ CD4⁺ cells, and representative proportions of IL17A⁺ CD4⁺ cells are shown. *, $P < 0.05$. For symbols, see key.

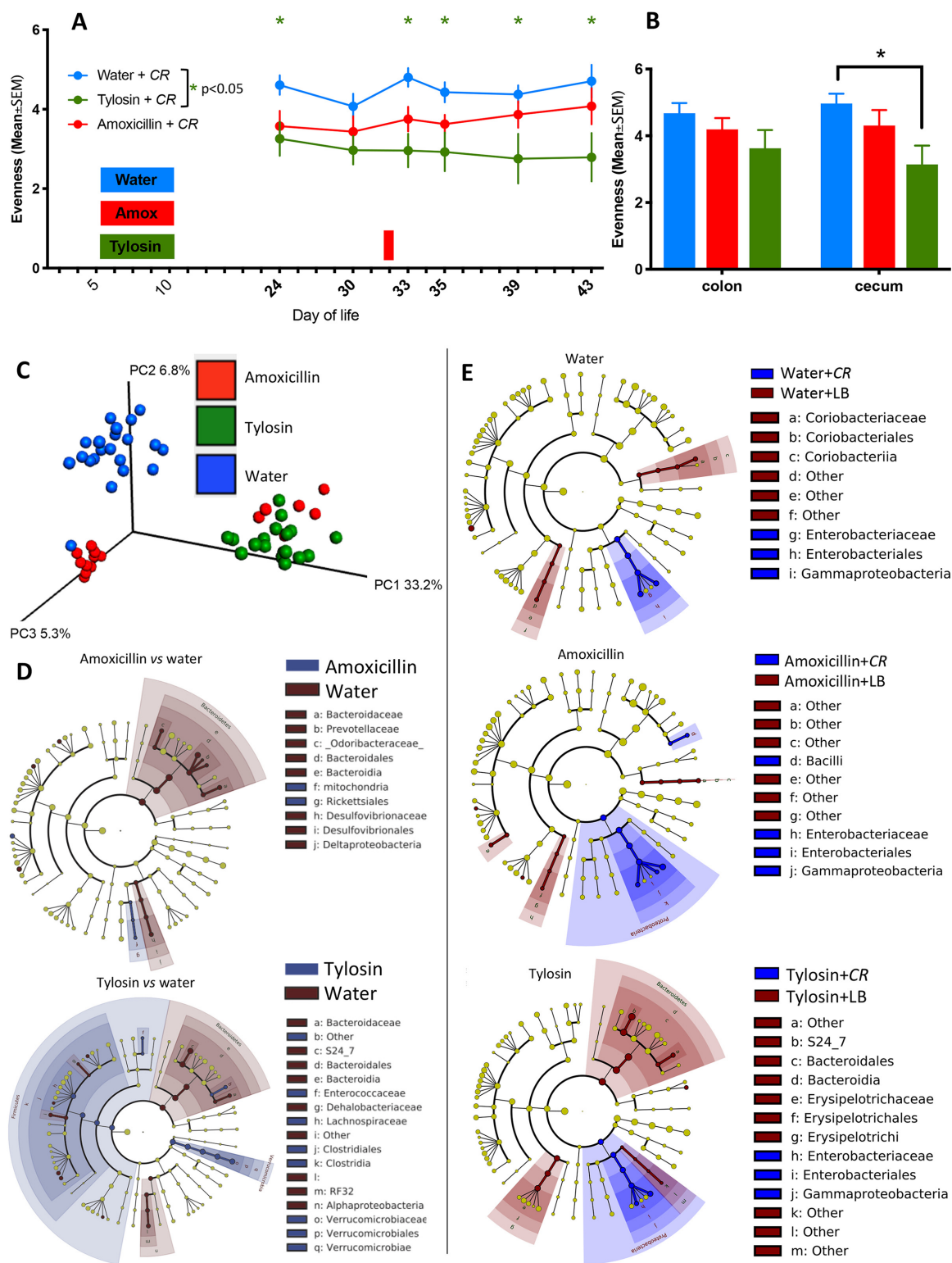


FIG 4 Gut microbiota characteristics of mice challenged with *C. rodentium* (or LB) 23 days after antibiotic or water exposure. (A) Study design (see the legend to Fig. 3A), with all samples obtained at sacrifice unless as noted. Fecal pellets were collected at the times shown in bold, and α -diversity using the Shannon index of evenness is shown. The red bar on the x axis corresponds to *C. rodentium* challenge. (B) α -Diversity in cecal and colonic samples using Shannon index of evenness. Samples were obtained 11 days after *C. rodentium* challenge from mice preexposed to water (blue), amoxicillin (red), or tylosin (green). *, $P < 0.05$. (C) Unweighted UniFrac analysis of fecal specimens visualized by PCoA (weaning, 2 days before challenge, and the day of challenge) for each group (for statistical significance, see Table S2). The three components explain 45.3% of the total variance. (D) LefSe analysis, with cladograms showing significantly differential taxa between indicated treatment groups on day 31 (2 days prior to *C. rodentium* challenge). Shading indicates significant overrepresentation (Continued on next page)

Downloaded from <http://mbio.asm.org/> on November 17, 2020 at INSERM

reveals that 23 days following cessation of the antibiotic exposure, the antibiotic-perturbed microbiota continues to be sufficient to enhance *C. rodentium*-induced colitis.

Mice exposed to early-life antibiotics had decreases in *Bacteroidia* that persisted up to 78 days postexposure. To determine whether specific bacterial species are associated with protection against *C. rodentium*, in two experiments we compared microbiota compositions between the antibiotic-exposed and control groups 21 days (Fig. 4D) and 78 days (Fig. 6B and C) after the exposure ended, in both cases immediately before the *C. rodentium* challenge. In both experiments, the antibiotic-exposed mice had reductions of *Bacteroidia* members (especially of the S24-7 family), and of *Alphaproteobacteria* and *Deltaproteobacteria* members (Fig. 4D and Fig. 6B and C); the effects of tylosin exposure were more pronounced than with amoxicillin, as reported previously (28). The S24-7 family was similarly depleted in the tylosin-perturbed inocula that had been used in the transfer studies (Fig. 8D). These results provide evidence associating *Bacteroidales* with protection against *C. rodentium*.

DISCUSSION

Antibiotic use, particularly in young children, is occurring at high levels (31, 36, 37). Perturbations of the microbiota induced by antibiotic exposure can be long term (38–41) and also can compromise host mucosal immunity (24). Both clinical and epidemiologic studies provide evidence that antibiotic use, especially in young children, increases susceptibility to gastrointestinal infections in the postantibiotic period (32, 42).

In this study, using a model system, we examined the effects of early-life antibiotic exposure on the host microbiota and on the course of bacterial colitis induced after antibiotic cessation. Since early life is critical to microbiota development in humans (43–45), and microbiota perturbations during this critical window may be more long lasting (46), we studied whether the durability of these effects is enhanced in mice exposed to antibiotics as pups.

Our first model involved mice exposed to tylosin as young adults and challenged with *C. rodentium* immediately after the course was completed. The resulting microbiota perturbations and more severe colitis were consistent with studies involving exposure to a different antibiotic (metronidazole) prior to *C. rodentium*-induced colitis (14) and with studies in the context of other antibiotic classes and other gastrointestinal pathogens (13, 47–49).

Since early-life antibiotic exposure induces long-term effects on host microbiota (28, 30), and microbiota composition directly influences the outcome of *C. rodentium* infection (22, 23), we asked whether susceptibility to *C. rodentium* represents another durable consequence of early-life antibiotic exposure. The antibiotics used in the current models—tylosin (macrolide) and amoxicillin (β -lactam)—represent the two classes of antibiotics most frequently prescribed to children (37). Moreover, they were dosed at levels that are therapeutic in mice (50–52) and consistent with recommendations for the treatment of acute infections in children (53, 54).

In agreement with our prior studies (28, 30), the microbiota perturbations induced by early-life antibiotics remained present up to the longest interval studied (now up to 80 days postexposure). The severity and durability of these perturbations were greater for the macrolide than the β -lactam, as reported for both mice (28) and children (38). That the tylosin-exposed mice developed more severe disease than the amoxicillin-exposed hosts links the extent of microbiota perturbation with colitis severity, a finding consistent with studies of postantibiotic gastroenteritis severity correlating with the antibiotic dose (47).

Although differences in mouse vendors and strains have been causally associated

FIG 4 Legend (Continued)

of the indicated taxa ($P < 0.05$; LDA > 2). (E) LefSe analysis between *C. rodentium* challenged (blue) and unchallenged (brown) mice on day 11 after challenge.

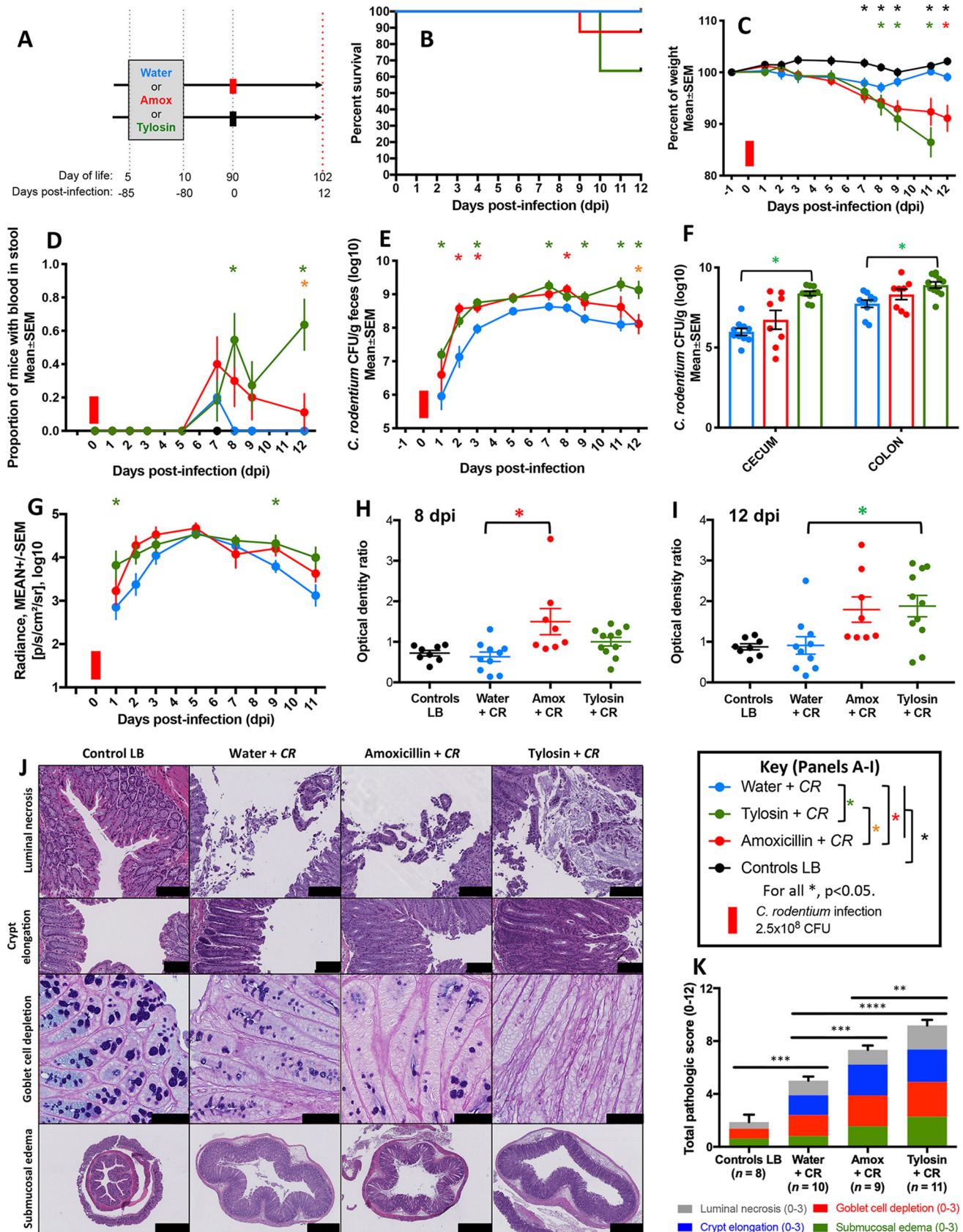


FIG 5 Characteristics of mice challenged with *C. rodentium* (or LB) 80 days after antibiotic or water exposure. (A) Study design. Five-day-old pups received a 5-day course of tylosin ($n = 14$), amoxicillin ($n = 13$), or water ($n = 12$). Eighty days later, pups were challenged with *luxCDABE C. rodentium* (water + CR (Continued on next page)

Downloaded from <http://mbio.asm.org/> on November 17, 2020 at INSERM

with interhost differences in *C. rodentium* infection susceptibility (22, 23), the enhanced colitis we observed could have directly resulted from immunomodulatory effects of macrolides early in life (55, 56) rather than from microbiota-mediated changes. Our transfer experiment examined that issue. Compared to control recipients, the microbiota in recipients of the tylosin-perturbed inocula showed diminished community richness and altered community structure persisting throughout the posttransfer period, highlighting the durability of the early-life tylosin-induced microbiota alterations (30). That the recipients of the antibiotic-perturbed inocula experienced more severe infection upon *C. rodentium* challenge than the control recipients confirms the causal role of the perturbed microbiota in worsening the colitis.

Multiple mechanisms may explain how the antibiotic-perturbed microbiota increases host susceptibility to *C. rodentium* infection. First, antibiotic-induced reductions in the total microbiota burden may directly enable *C. rodentium* to colonize at higher levels (57). However, total 16S microbial densities in mice exposed to early-life antibiotics return to normal almost immediately (30), indicating the importance of microbiota composition rather than number, especially for the remote challenges. *Proteobacteria* members known to compete with *C. rodentium* were reduced by antibiotics, which may facilitate its mucosal colonization (58). Antibiotics alter production of microbiota metabolites sensed by *C. rodentium*, like indole, which aid the organism in discriminating lumen and epithelial surfaces (59). Ampicillin exposure also decreases short-chain fatty acid (SCFA)-producing bacteria permitting *Enterobacteriaceae* expansion (7), providing another mechanism for colonization resistance.

Second, through altering microbiota composition, antibiotics may reduce goblet cell mucus production; a thinner mucus layer allows increased *C. rodentium* attachment to the epithelium (14, 60). The greater severity of *C. rodentium* colitis in mice genetically deficient in mucin production than in wild-type hosts highlights the protective importance of the mucus layer (57). However, regardless of mechanism, the effects of antibiotic exposure on mucus production should be immediate and short term; thus, a direct antibiotic role is not compatible with a model in which *C. rodentium* challenge occurs months after the early-life antibiotic exposure has ended. However, an indirect role of antibiotics in host mucus production—in which the antibiotic-perturbed microbiota serves as the intermediary factor—is consistent with our observations. We have confirmed that a single early-life antibiotic course led to long-lasting reductions of *Bacteroidales*—especially of the S24-7 family (29, 30), which are known to stimulate colonic mucus production (61), perhaps by recruiting interleukin 6 (IL-6)-producing intraepithelial lymphocytes (62). S24-7 family abundance has been associated with a more resistant mucus layer (63).

Third, by depleting the native microbiota, antibiotics may reduce production of IL-22 and antimicrobial peptides, which are important innate immune defenses against *C. rodentium* (23); however, a direct antibiotic role implies that these levels return to normal after the exposure ceases.

Fourth, early-life tylosin exposure decreases colonic T_H17 cells (30), as we reconfirmed, and in other experimental models, we found that the T_H17 cell reduction persisted for >24 days following a similar antibiotic exposure (C. Ozkul and V. Ruiz, unpublished data). That mice deficient in segmented filamentous bacteria (“*Candidatus* Savagella”), a commensal species that induces intestinal T_H17 cell differentiation, were

FIG 5 Legend (Continued)

[*n* = 10; blue], tylosin + CR [*n* = 11; green], and amoxicillin + CR [*n* = 10; red]) or with LB (water + LB [*n* = 2], tylosin + LB [*n* = 3], or amoxicillin + LB [*n* = 3]; black). (B) Percent surviving by exposure group. (C) Body weight over time, calculated as a percentage of prechallenge weight. For the tylosin group, analysis was censored at day 12 due to multiple deaths. (D) Proportion of mice with fecal occult blood. (E and F) Quantitation of *C. rodentium*, by culture, of feces (over time) and colon and cecum (at sacrifice). (G) Quantitation of *C. rodentium* by *in vivo* bioluminescent imaging. (H and I) Anti-*C. rodentium* IgM antibody levels 8 and 12 days postinfection (dpi), respectively. (J) Representative H&E-stained (or, in the third row, AB/PAS-stained) distal colonic sections (scale bars: for luminal necrosis, 100 μ m; for crypt elongation, 100 μ m; for goblet cell depletion, 50 μ m; and for submucosal edema, 500 μ m). (K) Cumulative histopathology scores (means \pm SEM), calculated by evaluating luminal necrosis, crypt elongation, goblet cell depletion, and submucosal edema. **, *P* < 0.01; ***, *P* < 0.001; ****, *P* < 0.0001. For symbols, see key.

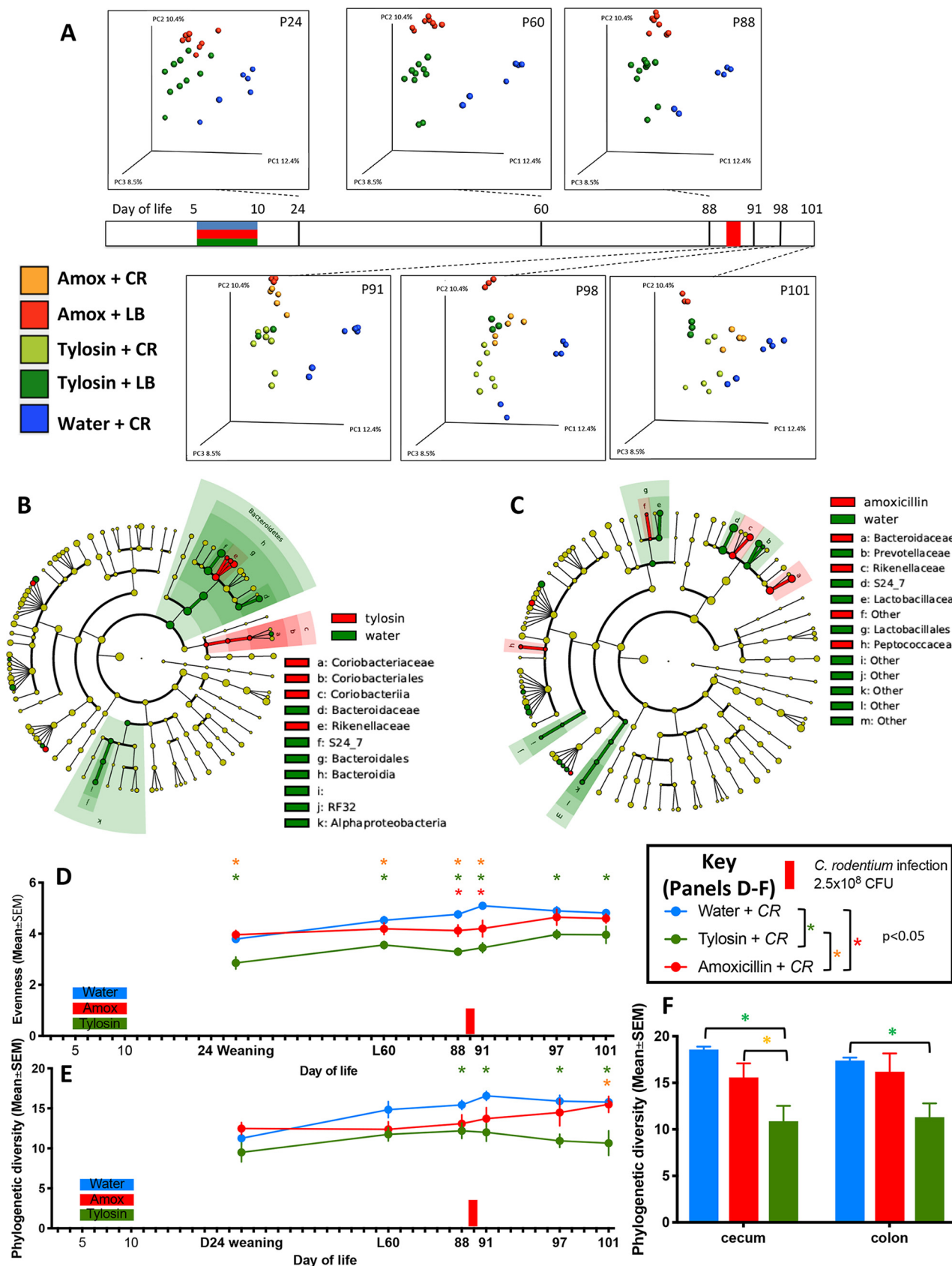


FIG 6 Gut microbiota characteristics of mice challenged with *C. rodentium* (or LB) 80 days after antibiotic or water exposure. (A) Study design (see the legend to Fig. 5A). Shown is an unweighted UniFrac analysis of fecal specimens visualized PCoA (for statistical significance, see Table S3). This cohort (Continued on next page)

more susceptible to *C. rodentium*-induced colitis underscores the importance of these cells in *C. rodentium* resistance (22).

Our study is limited, since although we have identified a causal role for early-life antibiotic-induced microbiota perturbation in the outcome of *C. rodentium* infection, we have not identified the exact mechanisms enabling *C. rodentium* to flourish. Our study also is limited to the effects of two antibiotics. While exposure to many antibiotic classes enhances *C. rodentium*-induced colitis, exposure to streptomycin does not (14), indicating that the selective effects on particular microbial taxa may be important. By suppressing susceptible organisms, streptomycin selects for *Bacteroidetes* and is protective in murine DSS (dextran sulfate sodium)-induced colitis, limiting *Enterobacteriaceae* blooms (64); although the ecological effects of streptomycin exposure are complex, that finding is consistent with a role of anaerobes in controlling *C. rodentium* populations.

Although we cannot exclude the possibility that early-life antibiotic exposure may reset immunological tone that directly leads to enhanced colitis susceptibility, the ability of the transferred microbiota to confer enhanced colitis indicates that the perturbed microbiota of early life is at least causally involved. Studies involving the transfer of immunocytes from antibiotic-exposed mice to immunodeficient mice will be required to test specific immunological hypotheses.

In conclusion, early-life antibiotic exposure in mice induces a long-lasting state of susceptibility to the consequences of *C. rodentium* infection. Extrapolating these results to humans suggests that antibiotic courses given to children may increase susceptibility to subsequent infections, even ones unrelated to those for which the antibiotic was prescribed (65). Restoring the critical species that were reduced or depleted by early-life antibiotics could alleviate such effects.

MATERIALS AND METHODS

Mice. Four separate experiments were conducted. The first experiment involved 21-day-old female C57BL6/J mice obtained from the Jackson Laboratory (Bar Harbor, ME). These mice were exposed to tylosin or water from days 27 to 32 of life (Fig. 1A). The second and third experiments involved 6-week-old male and female C57BL/6J obtained from the Jackson Laboratory, which were bred to produce litters of newborn pups. Mothers were exposed to amoxicillin, tylosin, or neither in their drinking water ($n = 6$, $n = 6$, and $n = 5$, respectively), and their pups were then exposed via their mother's milk ($n = 26$, $n = 27$, and $n = 27$, respectively). When pups reached 24 days of age, litters were weaned, and mice were separated by sex and by antibiotic treatment. In assembling the groups for challenge and follow-up, we maximized mixing of the pups between litters to minimize cage effects. Pups from these groups were then challenged with *C. rodentium* ($n = 10$ /treatment group) or LB (as a control; $n = 3$ /treatment group) either 23 days later (in the second experiment [Fig. 3A]) or 80 days later (in the third experiment [Fig. 5A]). The fourth experiment (Fig. 7A) involved wild-type C57BL/6 mice that were exposed to tylosin ($n = 2$) or water ($n = 2$) during days 5 to 10 of life (through their mother's milk), sacrificed at day 32 of life, and used as cecal content donors. Female germfree C57BL/6 mice at the age of 6 weeks ($n = 6$) were used as recipients of either tylosin-perturbed ($n = 3$) or control ($n = 3$) cecal contents. All mice were maintained on a 12-h light/dark cycle and allowed *ad libitum* access to food and water in a level 2 animal facility. Mice were sacrificed via carbon dioxide asphyxiation and cervical dislocation.

Ethics statement. All animal experimentation was approved by the New York University School of Medicine Institutional Animal Care and Use Committee (IACUC protocol no. S15-01484) in accordance with the National Institutes of Health's *Public Health Service Policy on Humane Care and Use of Laboratory Animals* (70) and the National Research Council of the National Academy of Sciences' *Guide for the Care and Use of Laboratory Animals* (71).

Antibiotic exposures. Tylosin tartrate and amoxicillin trihydrate (Sigma-Aldrich, St. Louis, MO) were dissolved in distilled deionized water at concentrations of 0.333 and 0.167 mg/ml, respectively. Mice were exposed to antibiotics through their drinking water or their mother's milk, as described previously (28, 30). The serum half-lives of tylosin and amoxicillin both are less than 1 h (28).

FIG 6 Legend (Continued)

excluded a group treated with water plus LB. The three components explain 31.3% of the total variance. (B and C) LefSe analysis, with cladograms showing significantly differential taxa between indicated treatment groups on day 88 (2 days prior to *C. rodentium* challenge). Shading indicates significant overrepresentation of the indicated taxa ($P < 0.05$; LDA > 2). (D and E) Fecal pellets were collected at the times shown in bold, and α -diversity using the phylogenetic diversity (PD whole tree) metric (D) or Shannon index of evenness (E) is shown. (F) Cecal and colonic contents were collected at sacrifice, and α -diversity using the phylogenetic diversity (PD whole tree) metric is shown. Samples were obtained 12 days after *C. rodentium* challenge from mice preexposed to water (blue), amoxicillin (red), or tylosin (green). For symbols, see key.

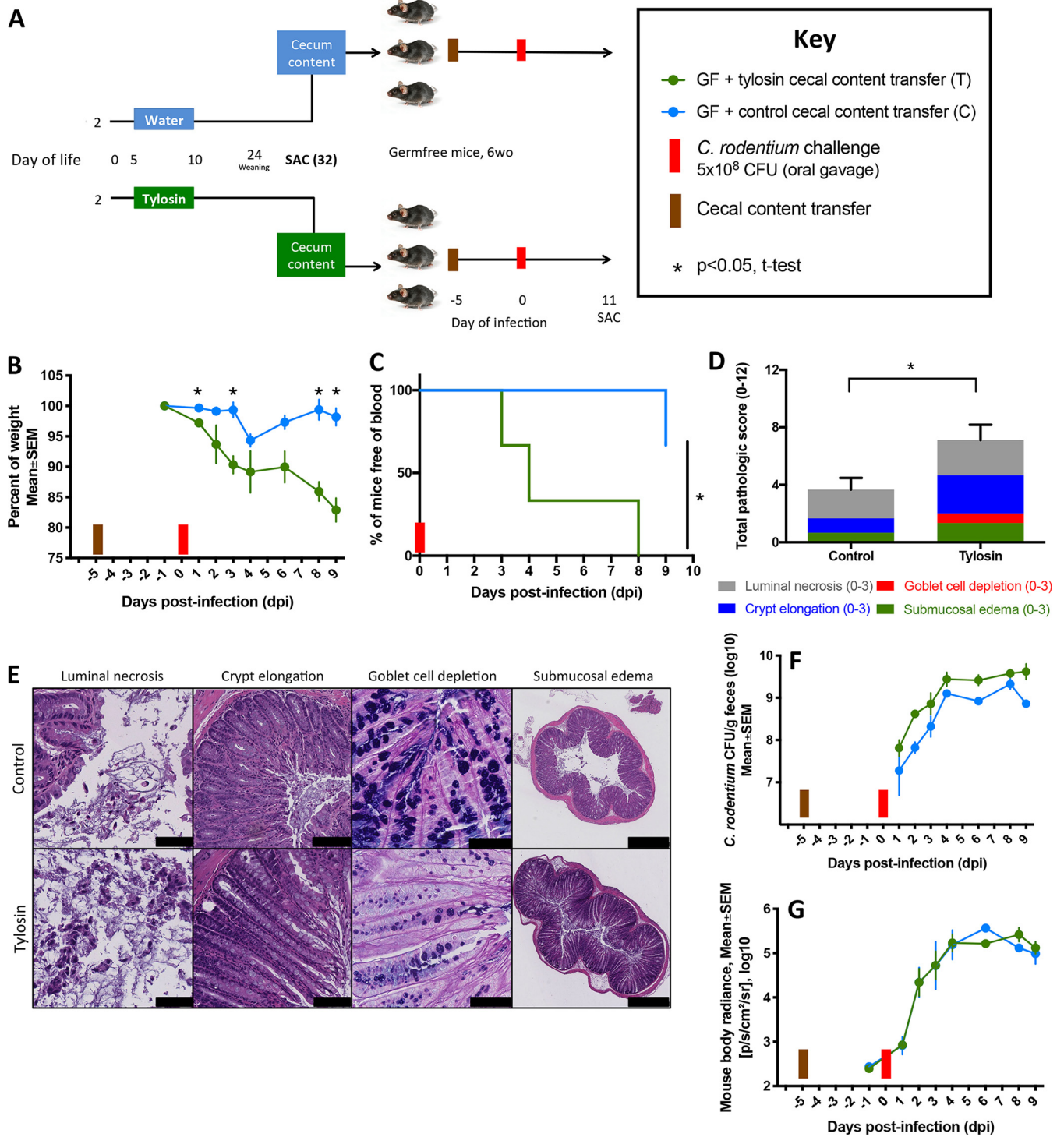


FIG 7 Transfer experiment: characteristics of recipient mice challenged with *C. rodentium* after gavage with tylosin-perturbed or control cecal contents. (A) Study design. Five-day-old conventionally raised mice received a 5-day course of tylosin ($n = 2$) or water ($n = 2$) and were sacrificed 22 days later. Cecal contents from these mice were transferred by gavage to 6-week-old germfree mice ($n = 3$ /group). Five days later, these recipient mice were challenged by *luxCDABE* *C. rodentium*. (B) Body weight over time, calculated as a percentage of prechallenge weight. (C) Kaplan-Meier curve assessed the occurrence of fecal occult blood. (D) Cumulative histopathology scores (means \pm SEM)—calculated by evaluating luminal necrosis, crypt elongation, goblet cell depletion, and submucosal edema—in the recipient mice gavaged with control or tylosin-perturbed cecal contents. (E) Representative H&E-stained (or, in the third column, AB/PAS-stained) distal colonic sections from recipient mice at sacrifice (scale bars: for luminal necrosis, 50 μ m; for crypt elongation, 100 μ m; for goblet cell depletion, 50 μ m; and for submucosal edema, 500 μ m). (F) Quantitation of *C. rodentium* in fecal culture. (G) Quantitation of *C. rodentium* by *in vivo* bioluminescent imaging. For symbols, see key.

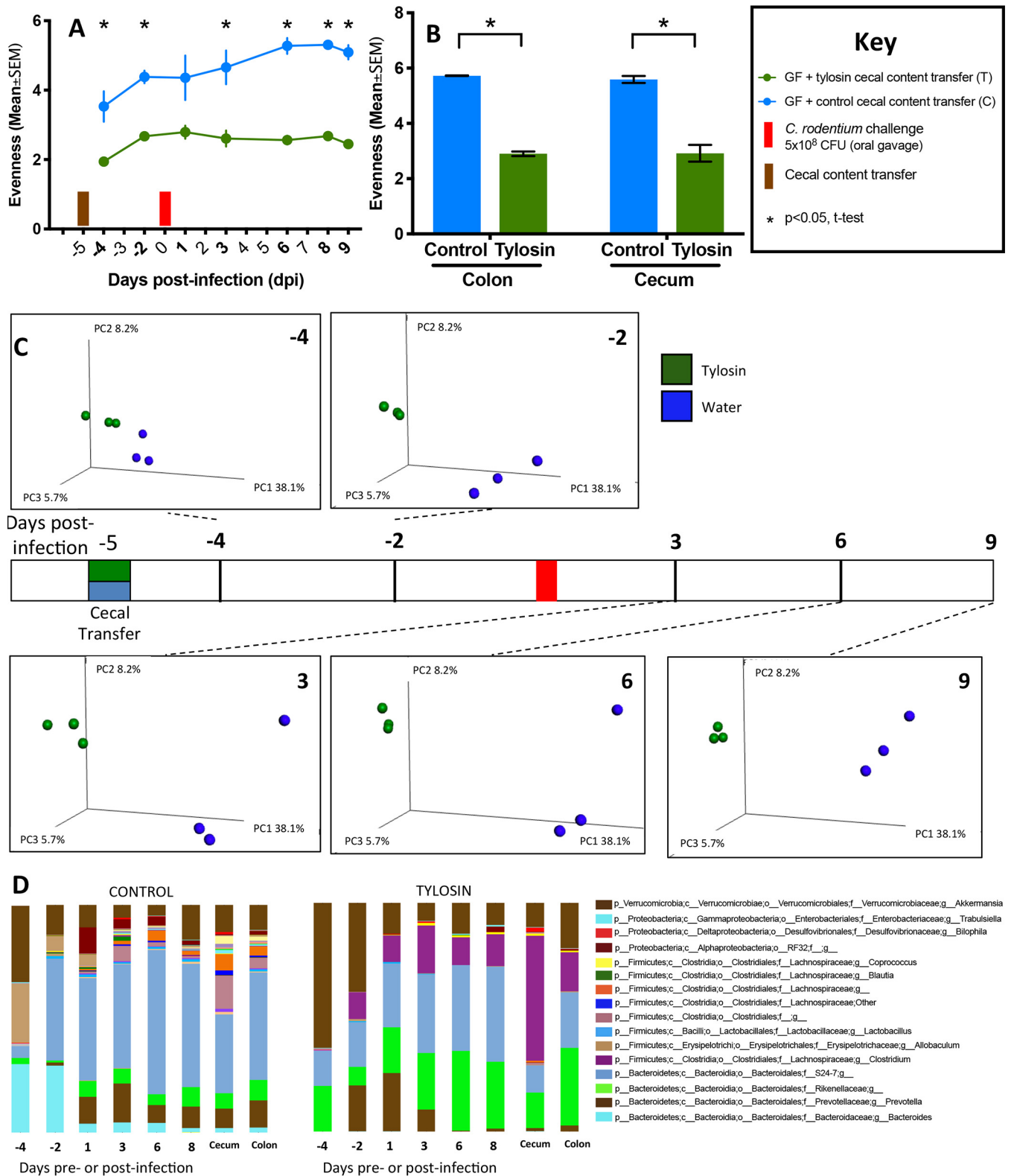


FIG 8 Transfer experiment: gut microbiota characteristics of recipient mice after gavage with tylosin-perturbed or control cecal contents and subsequent *C. rodentium* challenge. (A) Study design (see the legend to Fig. 7A). Fecal pellets were collected at the times shown in bold, and α -diversity using the Shannon index of evenness is shown. (B) α -Diversity of colonic and cecal contents at sacrifice using the Shannon index of evenness is shown. (C) Unweighted UniFrac analysis of fecal specimens visualized by PCoA. The three components explain 52% of the total variance. Statistical analysis of intergroup UniFrac distances was performed by Adonis test, with *P* values shown. (D) Relative abundances of taxa (present at >1% at the species level) in recipients of control or tylosin-perturbed cecal contents (control and tylosin, respectively). Days pre- or postinfection refer to fecal samples; cecum and colon were obtained at sacrifice. For symbols, see key.

Citrobacter rodentium infection. We used a bioluminescent strain of *C. rodentium* that contained a chromosomal promoterless *luxCDABE* operon from the nematode symbiont *Photorhabdus luminescens* and a kanamycin resistance cassette (pUTmini-Tn5 *luxKm2*) (72). A single *C. rodentium* colony was inoculated into Luria broth (LB) and grown overnight (at 37°C and 150 rpm). As confirmed by dilution plating, mice were challenged by oral gavage with 0.1 ml of LB containing between 2.5×10^8 and 5×10^8 CFU of *C. rodentium*.

To establish an enteric infection challenge model, we asked whether a single *C. rodentium* gavage was sufficient or whether two gavages was optimal. Since there were no significant differences between the two approaches in mouse weight, fecal occult blood, or *C. rodentium* quantitation (Fig. S1A to D), we used a single gavage in subsequent experiments. Mice also were monitored for morbidity and mortality following *C. rodentium* challenge. Mice were weighed every 2 days after challenge and were euthanized if signs of extreme distress (>20% loss of prechallenge body weight, hunched posture, inactivity, or seizure) were present. The presence of fecal occult blood was determined using Hemocult (Beckman Coulter, Indianapolis, IN). Fecal, cecal, and colonic specimens were collected and either diluted in phosphate-buffered saline (PBS) for *C. rodentium* quantitation or frozen at -80°C for microbiota analyses. Every other day during the postinfection period, mice were anesthetized with 2% isoflurane mixed with 2% oxygen, imaged using IVIS (PerkinElmer, Santa Clara, CA), and then returned to their cages after imaging. Images were analyzed with Living Image v4.5.2 software (PerkinElmer) (72), and the average radiance for each mouse was obtained.

Citrobacter rodentium quantitation. Fecal pellets collected from individual mice were weighed, homogenized in 1 ml of PBS with autoclaved beads, serially diluted, inoculated (in duplicate) on MacConkey agar plates containing kanamycin (50 mg/ml), and incubated at 37°C. Bacterial colonies were enumerated after 24 h.

Histopathological scoring. Formalin-fixed, paraffin-embedded distal colonic tissue sections (5 μ m) were obtained from mice upon sacrifice and were stained with hematoxylin and eosin (H&E) or with alcian blue (AB)/periodic acid-Schiff (PAS) (Poly Scientific R&D Corp., Bay Shore, NY) for goblet cell visualization. Stained slides were scanned for visualization on an SCN400F instrument (Leica Biosystems Inc, Buffalo Grove, IL). Tissue sections were scored, in a blinded fashion, using the following criteria adapted from similar studies (48, 60). Each criterion was scored on a scale of 0 to 3, for a maximum cumulative score of 12. The upper limits of the first, second, and third quartiles of the compiled measurements for criteria ii to iv were calculated and used as the thresholds for the minimum mean measurement required for a scaled score of 1, 2, or 3, respectively. Scored characteristics were as follows. (i) Luminal necrosis, i.e., the presence or density of necrotic epithelial cells in the lumen, was scored as follows: 0, absent; 1, scant; 2, moderate; and 3, dense. (ii) Crypt elongation, i.e., the heights of 20 well-oriented, randomly selected crypts, was measured, and the mean crypt length was scored as follows: 0, $\leq 209 \mu$ m; 1, 210 to 258 μ m; 2, 259 to 318 μ m; and 3, $\geq 319 \mu$ m. (iii) For goblet cell depletion, 16 high-power fields (HPFs) (rectangular fields of dimensions 210 μ m by 210 μ m) were randomly selected, as described previously (48); within each HPF, goblet cell numbers and volumes were calculated using ImageJ v1.50 software (73). The goblet cell counts per HPF were then normalized to the mean goblet cell volume, and the mean goblet cell count per HPF was scored as follows: 0, ≥ 74 ; 1, 39 to 73; 2, 15 to 38; and 3, ≤ 14 . (iv) For submucosal edema, the percent area of the intestinal wall occupied by the submucosa was calculated using ImageJ v1.50 software and scored as follows: 0, $\leq 3.2\%$; 1, 3.3 to 5.7%; 2, 5.8 to 9.3%; and 3, $\geq 9.4\%$.

Microbiota transfer. Cecal contents were collected from donor mice as described above and the contents divided, with half immediately immersed in prerduced anaerobic dental transport medium (Anaerobe Systems, Morgan Hill, CA) and then frozen at -80°C, as described previously (66). Upon thawing under anaerobic conditions, the cecal contents from 2 mice/group (tylosin preexposed or control) were pooled and further diluted in dental transport medium. Germfree mice received this suspension (150 μ l) via oral gavage and 5 days later were challenged by *C. rodentium*, as described above.

Determination of anti-Citrobacter rodentium antibody titers in serum. Peripheral blood was collected from mice before *C. rodentium* challenge, and at 8 and 11 dpi, by submandibular puncture. Blood samples were centrifuged at $2,000 \times g$ for 10 min and sera stored at -80°C. Specific antibodies to *C. rodentium* antigens were quantitated by enzyme-linked immunosorbent assay (ELISA) using a sonicated overnight culture of *C. rodentium* as the antigen source, and protein concentrations were measured using a bicinchoninic acid (BCA) protein assay kit (Fisher Scientific). All assays were performed in duplicate with positive and negative internal controls. The antigen was diluted in 0.5 M carbonate buffer (pH 9.6) for a protein concentration of 10 μ g/ml. Aliquots (0.1 ml) were added to wells of flat-bottom Immulon 2 plates (Dynatech Laboratories, Alexandria, VA) and incubated overnight at room temperature. Nonspecific binding was prevented by incubating plates with PBS buffer with 0.1% gelatin for 4 h at 37°C. After incubation, plates were washed 3 times and 0.1-ml volumes of serum samples diluted to 1:100 in PBS were added. After incubation at 37°C for 1 h, plates were washed 3 times and 0.1-ml volumes of peroxidase conjugates of goat anti-human IgG (Thermo Fisher, Waltham, MA) or IgM (Invitrogen) diluted to 1:1,000 were added. Horseradish peroxidase (HRP) substrate was added and the colorimetric reaction was quantified by MRX Revelation (Dynex Technologies, Chantilly, VA).

DNA extraction, library preparation, and microbial community analysis. DNA was extracted from fecal, cecal, and colonic specimens using a MoBio 96-well extraction kit. For amplicon library generation, the 16S rRNA V4 region was amplified with gene-specific primers, as described previously (66). The reverse amplification primers contained a 12-bp Golay barcode for multiplexed sequencing runs that

support pooling >1,000 samples. Amplicons were prepared in triplicate, pooled, and quantified. The 254-bp V4 region was sequenced using the Illumina MiSeq 2 × 150-bp platform. Operational taxonomic units (OTUs) were picked using an open reference picking strategy and Greengenes 13_8 for reference. Downstream processing of 16S rRNA sequences was performed using the QIIME 1.9.1 pipeline (67). Sequences were quality filtered with a Phred score of 20, chimeras were removed (ChimeraSlayer), and samples with a sequence depth of <600 were excluded. Filtered reads were clustered into 97% identity OTUs using the program UCLUST, followed by taxonomy assignment using the RDP Classifier. The phylogenetic tree and abundance tables generated were used to calculate unweighted and weighted UniFrac diversity indices. The OTU absolute-abundance tables were extracted from the pipeline for further analysis using the phyloseq package in the R statistical programming environment (68). Taxon compositions were compared using LefSe (69).

Isolation of colonic lamina propria lymphocytes. The large intestine was excised, placed in digestion medium containing 1 mM dithiothreitol (DTT) and 1 mM EDTA in calcium- and magnesium-free Hanks balanced salt solution (HBSS) supplemented with 2% fetal calf serum (FCS), and subsequently treated with collagenase IV-DNase digestion mix (0.5 mg/ml of collagenase IV and 200 μg/ml of DNase). Lymphocytes were enriched using a 40%/80% discontinuous Percoll (GE Lifesciences, Pittsburgh, PA) gradient. Lymphocytes derived from mesenteric lymph nodes were isolated through mechanical processing using a sterile 70-μm cell strainer (Corning, Corning, NY). Cells were stimulated with phorbol 12-myristate 13-acetate (PMA) and ionomycin for 4 h at 37°C in the presence of brefeldin A (GolgiPlug; BD Biosciences, San Jose, CA). Following stimulation, cells were stained with LIVE/DEAD fixable aqua (Thermo Fisher) and antibody-fluorophore combinations (i.e., allophycocyanin [APC]-Cy7-CD45, T cell receptor β [TCR-β]-fluorescein isothiocyanate [FITC], and CD4-V500 [BD Biosciences] and CD8-BV650, Foxp3-phycoerythrin [PE]-Cy7, IL-17-PE, and gamma interferon [IFN-γ]-FITC [eBioscience, San Diego, CA]) and then fixed with fix/perm (eBioscience) according to the manufacturer's instructions. Cells were acquired on an LSRII flow cytometer (BD Biosciences) and analyzed with FlowJo software (Tree Star, Ashland, OR); >100,000 events were collected for each sample. Samples with yields of <10,000 viable events were excluded from analysis.

Statistical analysis. Data are expressed as means ± standard errors of the means (SEM). Unless otherwise indicated, group means were compared by Kruskal-Wallis test with a *post hoc* test (Dunn's) for multiple comparisons, using Prism 8 software (GraphPad, La Jolla, CA).

SUPPLEMENTAL MATERIAL

Supplemental material for this article may be found at <https://doi.org/10.1128/mBio.02820-19>.

FIG S1, PDF file, 11.5 MB.

FIG S2, PDF file, 11.5 MB.

FIG S3, PDF file, 0.02 MB.

TABLE S1, DOCX file, 0.01 MB.

TABLE S2, DOCX file, 0.01 MB.

TABLE S3, DOCX file, 0.02 MB.

ACKNOWLEDGMENTS

We thank Ken Cadwell for providing germfree mice. We also thank the NYUMC Genome Technology Center for sequencing (cancer center support grant P30CA016087 at the Laura and Isaac Perlmutter Cancer Center).

Financial support was from the CHU Hôpitaux de Bordeaux, Philippe Foundation, Groupe Pasteur Mutualité, SGBSO (Société de gériatrie de Bordeaux et du Sud Ouest), NIH (U01 A122285), ASM Undergraduate Research Fellowship, C&D Fund, Zlinkoff Foundation, and Transatlantic Program of the Fondation Leducq.

The funders had no role in study design, data collection and interpretation, or the decision to submit the work for publication.

B.A.V. holds the CH.I.L.D. Foundation Chair in Pediatric Gastroenterology.

REFERENCES

- Schaedler RW, Dubos R, Costello R. 1965. The development of the bacterial flora in the gastrointestinal tract of mice. *J Exp Med* 122:59–66. <https://doi.org/10.1084/jem.122.1.59>.
- Savage DC, Dubos R, Schaedler RW. 1968. The gastrointestinal epithelium and its autochthonous bacterial flora. *J Exp Med* 127:67–76. <https://doi.org/10.1084/jem.127.1.67>.
- Gill SR, Pop M, Deboy RT, Eckburg PB, Turnbaugh PJ, Samuel BS, Gordon JI, Relman DA, Fraser-Liggett CM, Nelson KE. 2006. Metagenomic analysis of the human distal gut microbiome. *Science* 312:1355–1359. <https://doi.org/10.1126/science.1124234>.
- Ubeda C, Djukovic A, Isaac S. 2017. Roles of the intestinal microbiota in pathogen protection. *Clin Transl Immunology* 6:e128. <https://doi.org/10.1038/cti.2017.2>.
- Abt MC, Pamer EG. 2014. Commensal bacteria mediated defenses against pathogens. *Curr Opin Immunol* 29:16–22. <https://doi.org/10.1016/j.coi.2014.03.003>.
- Brown RL, Clarke TB. 2017. The regulation of host defences to infection by the microbiota. *Immunology* 150:1–6. <https://doi.org/10.1111/imm.12634>.
- Sorbara MT, Dubin K, Littmann ER, Moody TU, Fontana E, Seok R, Leiner

- IM, Taur Y, Peled JU, van den Brink MRM, Litvak Y, Baumler AJ, Chaubard JL, Pickard AJ, Cross JR, Pamer EG. 2019. Inhibiting antibiotic-resistant Enterobacteriaceae by microbiota-mediated intracellular acidification. *J Exp Med* 216:84–98. <https://doi.org/10.1084/jem.20181639>.
8. Savage DC, Dubos R. 1968. Alterations in the mouse cecum and its flora produced by antibacterial drugs. *J Exp Med* 128:97–110. <https://doi.org/10.1084/jem.128.1.97>.
 9. Modi SR, Collins JJ, Relman DA. 2014. Antibiotics and the gut microbiota. *J Clin Invest* 124:4212–4218. <https://doi.org/10.1172/JCI72333>.
 10. Bohnhoff M, Drake BL, Miller CP. 1954. Effect of streptomycin on susceptibility of intestinal tract to experimental Salmonella infection. *Proc Soc Exp Biol Med* 86:132–137. <https://doi.org/10.3181/00379727-86-21030>.
 11. Miller CP, Bohnhoff M, Rifkind D. 1956. The effect of an antibiotic on the susceptibility of the mouse's intestinal tract to Salmonella infection. *Trans Am Clin Climatol Assoc* 68:51–55; discussion, 55–58.
 12. Debast SB, Bauer MP, Kuijper EJ. 2014. European Society of Clinical Microbiology and Infectious Diseases: update of the treatment guidance document for Clostridium difficile infection. *Clin Microbiol Infect* 20(Suppl 2):1–26. <https://doi.org/10.1111/1469-0691.12418>.
 13. Becattini S, Littmann ER, Carter RA, Kim SG, Morjaria SM, Ling L, Gyaltsen Y, Fontana E, Taur Y, Leiner IM, Pamer EG. 2017. Commensal microbes provide first line defense against Listeria monocytogenes infection. *J Exp Med* 214:1973–1989. <https://doi.org/10.1084/jem.20170495>.
 14. Wlodarska M, Willing B, Keeney KM, Menendez A, Bergstrom KS, Gill N, Russell SL, Vallance BA, Finlay BB. 2011. Antibiotic treatment alters the colonic mucus layer and predisposes the host to exacerbated Citrobacter rodentium-induced colitis. *Infect Immun* 79:1536–1545. <https://doi.org/10.1128/IAI.01104-10>.
 15. Schauer DB, Falkow S. 1993. Attaching and effacing locus of a Citrobacter freundii biotype that causes transmissible murine colonic hyperplasia. *Infect Immun* 61:2486–2492.
 16. Collins JW, Keeney KM, Crepin VF, Rathinam VA, Fitzgerald KA, Finlay BB, Frankel G. 2014. Citrobacter rodentium: infection, inflammation and the microbiota. *Nat Rev Microbiol* 12:612–623. <https://doi.org/10.1038/nrmicro3315>.
 17. Eckmann L. 2006. Animal models of inflammatory bowel disease: lessons from enteric infections. *Ann N Y Acad Sci* 1072:28–38. <https://doi.org/10.1196/annals.1326.008>.
 18. Mundy R, MacDonald TT, Dougan G, Frankel G, Wiles S. 2005. Citrobacter rodentium of mice and man. *Cell Microbiol* 7:1697–1706. <https://doi.org/10.1111/j.1462-5822.2005.00625.x>.
 19. Maaser C, Housley MP, Iimura M, Smith JR, Vallance BA, Finlay BB, Schreiber JR, Varki NM, Kagnoff MF, Eckmann L. 2004. Clearance of Citrobacter rodentium requires B cells but not secretory immunoglobulin A (IgA) or IgM antibodies. *Infect Immun* 72:3315–3324. <https://doi.org/10.1128/IAI.72.6.3315-3324.2004>.
 20. Vallance BA, Deng W, Jacobson K, Finlay BB. 2003. Host susceptibility to the attaching and effacing bacterial pathogen Citrobacter rodentium. *Infect Immun* 71:3443–3453. <https://doi.org/10.1128/iai.71.6.3443-3453.2003>.
 21. Ghosh S, Dai C, Brown K, Rajendiran E, Makarenko S, Baker J, Ma C, Halder S, Montero M, Ionescu VA, Klegeris A, Vallance BA, Gibson DL. 2011. Colonic microbiota alters host susceptibility to infectious colitis by modulating inflammation, redox status, and ion transporter gene expression. *Am J Physiol Gastrointest Liver Physiol* 301:G39–G49. <https://doi.org/10.1152/ajpgi.00509.2010>.
 22. Ivanov II, Atarashi K, Manel N, Brodie EL, Shima T, Karaoz U, Wei D, Goldfarb KC, Santee CA, Lynch SV, Tanoue T, Imaoka A, Itoh K, Takeda K, Umesaki Y, Honda K, Littman DR. 2009. Induction of intestinal Th17 cells by segmented filamentous bacteria. *Cell* 139:485–498. <https://doi.org/10.1016/j.cell.2009.09.033>.
 23. Willing BP, Vacharaksa A, Croxen M, Thanachayanont T, Finlay BB. 2011. Altering host resistance to infections through microbial transplantation. *PLoS One* 6:e26988. <https://doi.org/10.1371/journal.pone.0026988>.
 24. Willing BP, Russell SL, Finlay BB. 2011. Shifting the balance: antibiotic effects on host-microbiota mutualism. *Nat Rev Microbiol* 9:233–243. <https://doi.org/10.1038/nrmicro2536>.
 25. Mullineaux-Sanders C, Collins JW, Ruano-Gallego D, Levy M, Pevsner-Fischer M, Glegola-Madejska IT, Sägfors AM, Wong JLC, Elinav E, Crepin VF, Frankel G. 2017. Citrobacter rodentium relies on commensals for colonization of the colonic mucosa. *Cell Rep* 21:3381–3389. <https://doi.org/10.1016/j.celrep.2017.11.086>.
 26. Martinez I, Maldonado-Gomez MX, Gomes-Neto JC, Kittana H, Ding H, Schmalz R, Joglekar P, Cardona RJ, Marsteller NL, Kembel SW, Benson AK, Peterson DA, Ramer-Tait AE, Walter J. 2018. Experimental evaluation of the importance of colonization history in early-life gut microbiota assembly. *Elife* 7:e36521. <https://doi.org/10.7554/eLife.36521>.
 27. Stewart CJ, Ajami NJ, O'Brien JL, Hutchinson DS, Smith DP, Wong MC, Ross MC, Lloyd RE, Doddapaneni H, Metcalf GA, Muzny D, Gibbs RA, Vatanen T, Huttenhower C, Xavier RJ, Rewers M, Hagopian W, Toppari J, Ziegler A-G, She J-X, Akolkar B, Lernmark A, Hyoty H, Vehik K, Krischer JP, Petrosino JF. 2018. Temporal development of the gut microbiome in early childhood from the TEDDY study. *Nature* 562:583–588. <https://doi.org/10.1038/s41586-018-0617-x>.
 28. Nobel YR, Cox LM, Kirigin FF, Bokulich NA, Yamanishi S, Teitler I, Chung J, Sohn J, Barber CM, Goldfarb DS, Raju K, Abubucker S, Zhou Y, Ruiz VE, Li H, Mitreva M, Alekseyenko AV, Weinstock GM, Sodergren E, Blaser MJ. 2015. Metabolic and metagenomic outcomes from early-life pulsed antibiotic treatment. *Nat Commun* 6:7486. <https://doi.org/10.1038/ncomms8486>.
 29. Zhang XS, Li J, Krautkramer KA, Badri M, Battaglia T, Borbet TC, Koh H, Ng S, Sibley RA, Li Y, Pathmasiri W, Jindal S, Shields-Cutler RR, Hillmann B, Al-Ghalith GA, Ruiz VE, Livanos A, van 'T Wout AB, Nagalingam N, Rogers AB, Sumner SJ, Knights D, Denu JM, Li H, Ruggles KV, Bonneau R, Williamson RA, Rauch M, Blaser MJ. 2018. Antibiotic-induced acceleration of type 1 diabetes alters maturation of innate intestinal immunity. *Elife* 7:e37816. <https://doi.org/10.7554/eLife.37816>.
 30. Ruiz VE, Battaglia T, Kurtz ZD, Bijmans L, Ou A, Engstrand I, Zheng X, Iizumi T, Mullins BJ, Muller CL, Cadwell K, Bonneau R, Perez-Perez GI, Blaser MJ. 2017. A single early-in-life macrolide course has lasting effects on murine microbial network topology and immunity. *Nat Commun* 8:518. <https://doi.org/10.1038/s41467-017-00531-6>.
 31. Rogawski ET, Platts-Mills JA, Seidman JC, John S, Mahfuz M, Ulak M, Shrestha SK, Soofi SB, Yori PP, Mduma E, Svendsen E, Ahmed T, Lima AA, Bhutta ZA, Kosek MN, Lang DR, Gottlieb M, Zaidi AK, Kang G, Bessong PO, Houpt ER, Guerrant RL. 2017. Use of antibiotics in children younger than two years in eight countries: a prospective cohort study. *Bull World Health Organ* 95:49–61. <https://doi.org/10.2471/BLT.16.176123>.
 32. Rogawski ET, Westreich D, Becker-Dreps S, Adair LS, Sandler RS, Sarkar R, Kattula D, Ward HD, Meshnick SR, Kang G. 2015. The effect of early life antibiotic exposures on diarrheal rates among young children in Vellore, India. *Pediatr Infect Dis J* 34:583–588. <https://doi.org/10.1097/INF.0000000000000679>.
 33. Man WH, Clerc M, de Steenhuijsen Piters WAA, van Houten MA, Chu M, Kool J, Keijser BJF, Sanders EAM, Bogaert D. 2019. Loss of microbial topography between oral and nasopharyngeal microbiota and development of respiratory infections early in life. *Am J Respir Crit Care Med* 200:760. <https://doi.org/10.1164/rccm.201810-1993OC>.
 34. Hoffmann C, Hill DA, Minkah N, Kirn T, Troy A, Artis D, Bushman F. 2009. Community-wide response of the gut microbiota to enteropathogenic Citrobacter rodentium infection revealed by deep sequencing. *Infect Immun* 77:4668–4678. <https://doi.org/10.1128/IAI.00493-09>.
 35. Jin S, Zhao D, Cai C, Song D, Shen J, Xu A, Qiao Y, Ran Z, Zheng Q. 2017. Low-dose penicillin exposure in early life decreases Th17 and the susceptibility to DSS colitis in mice through gut microbiota modification. *Sci Rep* 7:43662. <https://doi.org/10.1038/srep43662>.
 36. Hicks LA, Bartoces MG, Roberts RM, Suda KJ, Hunkler RJ, Taylor TH, Jr, Schrag SJ. 2015. US outpatient antibiotic prescribing variation according to geography, patient population, and provider specialty in 2011. *Clin Infect Dis* 60:1308–1316.
 37. Hersh AL, Shapiro DJ, Pavia AT, Shah SS. 2011. Antibiotic prescribing in ambulatory pediatrics in the United States. *Pediatrics* 128:1053–1061. <https://doi.org/10.1542/peds.2011-1337>.
 38. Korpela K, Salonen A, Virta LJ, Kekkonen RA, Forslund K, Bork P, de Vos WM. 2016. Intestinal microbiome is related to lifetime antibiotic use in Finnish pre-school children. *Nat Commun* 7:10410. <https://doi.org/10.1038/ncomms10410>.
 39. Jernberg C, Lofmark S, Edlund C, Jansson JK. 2007. Long-term ecological impacts of antibiotic administration on the human intestinal microbiota. *ISME J* 1:56–66. <https://doi.org/10.1038/ismej.2007.3>.
 40. Jakobsson HE, Jernberg C, Andersson AF, Sjolund-Karlsson M, Jansson JK, Engstrand L. 2010. Short-term antibiotic treatment has differing long-term impacts on the human throat and gut microbiome. *PLoS One* 5:e9836. <https://doi.org/10.1371/journal.pone.0009836>.
 41. Mangin I, Leveque C, Magne F, Suau A, Pochart P. 2012. Long-term changes in human colonic Bifidobacterium populations induced by a 5-day oral amoxicillin-clavulanic acid treatment. *PLoS One* 7:e50257. <https://doi.org/10.1371/journal.pone.0050257>.

42. Ryan CA, Nickels MK, Hargrett-Bean NT, Potter ME, Endo T, Mayer L, Langkop CW, Gibson C, McDonald RC, Kenney RT, Puhar ND, McDonnell PJ, Martin RJ, Cohen ML, Blake PA. 1987. Massive outbreak of antimicrobial-resistant salmonellosis traced to pasteurized milk. *JAMA* 258:3269–3274. <https://doi.org/10.1001/jama.1987.03400220069039>.
43. Yatsunen T, Rey FE, Manary MJ, Trehan I, Dominguez-Bello MG, Contreras M, Magris M, Hidalgo G, Baldassano RN, Anokhin AP, Heath AC, Warner B, Reeder J, Kuczynski J, Caporaso JG, Lozupone CA, Lauber C, Clemente JC, Knights D, Knight R, Gordon JI. 2012. Human gut microbiome viewed across age and geography. *Nature* 486:222–227. <https://doi.org/10.1038/nature11053>.
44. Bäckhed F, Roswall J, Peng Y, Feng Q, Jia H, Kovatcheva-Datchary P, Li Y, Xia Y, Xie H, Zhong H, Khan MT, Zhang J, Li J, Xiao L, Al-Aama J, Zhang D, Lee YS, Kotowska D, Colding C, Tremaroli V, Yin Y, Bergman S, Xu X, Madsen L, Kristiansen K, Dahlgren J, Wang J, Jun W. 2015. Dynamics and stabilization of the human gut microbiome during the first year of life. *Cell Host Microbe* 17:690–703. <https://doi.org/10.1016/j.chom.2015.04.004>.
45. Yassour M, Vatanen T, Siljander H, Hamalainen AM, Harkonen T, Ryhanen SJ, Franzosa EA, Vlamakis H, Huttenhower C, Gevers D, Lander ES, Knip M, Group DS, Xavier RJ. 2016. Natural history of the infant gut microbiome and impact of antibiotic treatment on bacterial strain diversity and stability. *Sci Transl Med* 8:343ra81. <https://doi.org/10.1126/scitranslmed.aad0917>.
46. Bokulich NA, Chung J, Battaglia T, Henderson N, Jay M, Li H, A DL, Wu F, Perez-Perez GI, Chen Y, Schweizer W, Zheng X, Contreras M, Dominguez-Bello MG, Blaser MJ. 2016. Antibiotics, birth mode, and diet shape microbiome maturation during early life. *Sci Transl Med* 8:343ra82. <https://doi.org/10.1126/scitranslmed.aad7121>.
47. Sekirov I, Tam NM, Jogova M, Robertson ML, Li Y, Lupp C, Finlay BB. 2008. Antibiotic-induced perturbations of the intestinal microbiota alter host susceptibility to enteric infection. *Infect Immun* 76:4726–4736. <https://doi.org/10.1128/IAI.00319-08>.
48. Barthel M, Hapfelmeier S, Quintanilla-Martínez L, Kremer M, Rohde M, Hogardt M, Pfeffer K, Rüssmann H, Hardt W-D. 2003. Pretreatment of mice with streptomycin provides a *Salmonella enterica* serovar Typhimurium colitis model that allows analysis of both pathogen and host. *Infect Immun* 71:2839–2858. <https://doi.org/10.1128/iai.71.5.2839-2858.2003>.
49. Buffie CG, Jarchum I, Equinda M, Lipuma L, Gobourne A, Viale A, Ubeda C, Xavier J, Pamer EG. 2012. Profound alterations of intestinal microbiota following a single dose of clindamycin results in sustained susceptibility to *Clostridium difficile*-induced colitis. *Infect Immun* 80:62–73. <https://doi.org/10.1128/IAI.05496-11>.
50. Andes D, Craig WA. 1998. In vivo activities of amoxicillin and amoxicillin-clavulanate against *Streptococcus pneumoniae*: application to breakpoint determinations. *Antimicrob Agents Chemother* 42:2375–2379. <https://doi.org/10.1128/AAC.42.9.2375>.
51. Du X, Li C, Sun HK, Nightingale CH, Nicolau DP. 2005. A sensitive assay of amoxicillin in mouse serum and broncho-alveolar lavage fluid by liquid-liquid extraction and reversed-phase HPLC. *J Pharm Biomed Anal* 39:648–652. <https://doi.org/10.1016/j.jpba.2005.04.021>.
52. Lewicki J. 2006. Tylosin: a review of pharmacokinetics, residues in food animals and analytical methods. United Nations Food and Agriculture Organization, Rome, Italy.
53. Fonseca W, Hoppu K, Rey LC, Amaral J, Qazi S. 2003. Comparing pharmacokinetics of amoxicillin given twice or three times per day to children older than 3 months with pneumonia. *Antimicrob Agents Chemother* 47:997–1001. <https://doi.org/10.1128/aac.47.3.997-1001.2003>.
54. Nahata MC, Koranyi KI, Luke DR, Foulds G. 1995. Pharmacokinetics of azithromycin in pediatric patients with acute otitis media. *Antimicrob Agents Chemother* 39:1875–1877. <https://doi.org/10.1128/aac.39.8.1875>.
55. Iwanaga N, Nakamura S, Oshima K, Kajihara T, Takazono T, Miyazaki T, Izumikawa K, Yanagihara K, Sugawara A, Sunazuka T, Omura S, Kohno S. 2015. Macrolides promote CCL2-mediated macrophage recruitment and clearance of nasopharyngeal pneumococcal colonization in mice. *J Infect Dis* 212:1150–1159. <https://doi.org/10.1093/infdis/jiv157>.
56. Ratzinger F, Haslacher H, Poepl W, Hoermann G, Kovarik JJ, Jutz S, Steinberger P, Burgmann H, Pickl WF, Schmetterer KG. 2014. Azithromycin suppresses CD4(+) T-cell activation by direct modulation of mTOR activity. *Sci Rep* 4:7438. <https://doi.org/10.1038/srep07438>.
57. Bergstrom KS, Kisson-Singh V, Gibson DL, Ma C, Montero M, Sham HP, Ryz N, Huang T, Velcich A, Finlay BB, Chadee K, Vallance BA. 2010. Muc2 protects against lethal infectious colitis by disassociating pathogenic and commensal bacteria from the colonic mucosa. *PLoS Pathog* 6:e1000902. <https://doi.org/10.1371/journal.ppat.1000902>.
58. Kamada N, Kim YG, Sham HP, Vallance BA, Puente JL, Martens EC, Nunez G. 2012. Regulated virulence controls the ability of a pathogen to compete with the gut microbiota. *Science* 336:1325–1329. <https://doi.org/10.1126/science.1222195>.
59. Kumar A, Sperandio V. 2019. Indole signaling at the host-microbiota-pathogen interface. *mBio* 10:e01031-19. <https://doi.org/10.1128/mBio.01031-19>.
60. Wlodarska M, Thaiss CA, Nowarski R, Henao-Mejia J, Zhang JP, Brown EM, Frankel G, Levy M, Katz MN, Philbrick WM, Elinav E, Finlay BB, Flavell RA. 2014. NLRP6 inflammasome orchestrates the colonic host-microbial interface by regulating goblet cell mucus secretion. *Cell* 156:1045–1059. <https://doi.org/10.1016/j.cell.2014.01.026>.
61. Burger-van Paassen N, Vincent A, Puiman PJ, van der Sluis M, Bouma J, Boehm G, van Goudoever JB, van Seuningen I, Renes IB. 2009. The regulation of intestinal mucin MUC2 expression by short-chain fatty acids: implications for epithelial protection. *Biochem J* 420:211–219. <https://doi.org/10.1042/BJ20082222>.
62. Kuhn KA, Schulz HM, Regner EH, Severs EL, Hendrickson JD, Mehta G, Whitney AK, Ir D, Ohri N, Robertson CE, Frank DN, Campbell EL, Colgan SP. 2018. Bacteroidales recruit IL-6-producing intraepithelial lymphocytes in the colon to promote barrier integrity. *Mucosal Immunol* 11:357–368. <https://doi.org/10.1038/mi.2017.55>.
63. Jakobsson HE, Rodriguez-Pineiro AM, Schutte A, Ermund A, Boysen P, Bemark M, Sommer F, Backhed F, Hansson GC, Johansson ME. 2015. The composition of the gut microbiota shapes the colon mucus barrier. *EMBO Rep* 16:164–177. <https://doi.org/10.15252/embr.201439263>.
64. Huang YL, Chassard C, Hausmann M, von Itzstein M, Hentzel T. 2015. Sialic acid catabolism drives intestinal inflammation and microbial dysbiosis in mice. *Nat Commun* 6:8141. <https://doi.org/10.1038/ncomms9141>.
65. Unger SA, Bogaert D. 2017. The respiratory microbiome and respiratory infections. *J Infect* 74(Suppl 1):S84–S88. [https://doi.org/10.1016/S0163-4453\(17\)30196-2](https://doi.org/10.1016/S0163-4453(17)30196-2).
66. Cox LM, Yamanishi S, Sohn J, Alekseyenko AV, Leung JM, Cho I, Kim SG, Li H, Gao Z, Mahana D, Zarate Rodriguez JG, Rogers AB, Robine N, Loke P, Blaser MJ. 2014. Altering the intestinal microbiota during a critical developmental window has lasting metabolic consequences. *Cell* 158:705–721. <https://doi.org/10.1016/j.cell.2014.05.052>.
67. Caporaso JG, Kuczynski J, Stombaugh J, Bittinger K, Bushman FD, Costello EK, Fierer N, Pena AG, Goodrich JK, Gordon JI, Huttley GA, Kelley ST, Knights D, Koenig JE, Ley RE, Lozupone CA, McDonald D, Muegge BD, Pirrung M, Reeder J, Sevinsky JR, Turnbaugh PJ, Walters WA, Widmann J, Yatsunen T, Zaneveld J, Knight R. 2010. QIIME allows analysis of high-throughput community sequencing data. *Nat Methods* 7:335–336. <https://doi.org/10.1038/nmeth.f.303>.
68. R Development Core Team. 2010. R Foundation for environment statistical computing. R Foundation for Statistical Computing, Vienna, Austria. Retrieved from <https://www.r-project.org/>.
69. Segata N, Izard J, Waldron L, Gevers D, Miropolsky L, Garrett WS, Huttenhower C. 2011. Metagenomic biomarker discovery and explanation. *Genome Biol* 12:R60. <https://doi.org/10.1186/gb-2011-12-6-r60>.
70. National Institutes of Health. 2015. Public Health Service policy on humane care and use of laboratory animals. Office of Laboratory Animal Welfare, National Institutes of Health, Bethesda, MD.
71. National Research Council. 2011. Guide for the care and use of laboratory animals, 8th ed. National Academies Press, Washington, DC.
72. Gibson DL, Ma C, Bergstrom KS, Huang JT, Man C, Vallance BA. 2008. MyD88 signalling plays a critical role in host defence by controlling pathogen burden and promoting epithelial cell homeostasis during *Citrobacter rodentium*-induced colitis. *Cell Microbiol* 10:618–631. <https://doi.org/10.1111/j.1462-5822.2007.01071.x>.
73. Schneider CA, Rasband WS, Eliceiri KW. 2012. NIH Image to ImageJ: 25 years of image analysis. *Nat Methods* 9:671–675. <https://doi.org/10.1038/nmeth.2089>.